Volume 24, No 4 | International Journal of Radiation Research, October 2026

Clinical value of ultrasound elastography combined with MRI T2 mapping in evaluating the invasiveness of giant cell tumor of tendon sheath

M. Chen[1#], Y. Jiang[2#], Q. Chen[1*]

[1]Department of Radiology, Wuxi Ninth People's Hospital Affiliated to Soochow University, Wuxi, Jiangsu, China
[2]Department of Radiology, The People's Hospital of Danyang; Affiliated Danyang Hospital of Nantong University, Danyang, Jiangsu, China

► ***Original article***

***Corresponding author:**
Qilong Chen, M.D.,
***E-mail:** wxchenqilong@163.com*

Received: January 2026
Final revised: April 2026
Accepted: May 2026

Int. J. Radiat. Res., October 2026; 24(4): 1061-1067

DOI: 10.61186/ijrr.24.4.17

Keywords: *Giant cell tumor of tendon sheath, elasticity imaging techniques, T2 mapping, neoplasm invasiveness, diagnostic accuracy, preoperative period.*

[#]These authors contributed to the work equally and should be regarded as co-first authors.

ABSTRACT

Background: Giant cell tumor of tendon sheath (GCTTS) is a common soft tissue tumor of the hand and periarticular regions. Although benign, it exhibits notable invasiveness. Accurate preoperative assessment of its invasiveness is crucial for improving surgical outcomes. Objective: To investigate the clinical value of ultrasound elastography (USE) combined with MRI T2 mapping in evaluating GCTTS invasiveness, providing objective evidence for preoperative diagnosis. ***Materials and Methods:*** From January 2021 to December 2025, 82 patients with suspected GCTTS at our hospital were selected and subjected to preoperative USE and MRI T2 mapping. They were divided into an invasive group (38 cases) and a non-invasive group (44 cases) based on postoperative pathological results. The imaging parameters of the two groups were compared. The cutoff values were determined using the receiver operating characteristic (ROC) curves, and the diagnostic performance of single and combined examinations was analyzed. ***Results:*** The maximum tumor diameter was closely related to invasiveness, with an invasion rate of 100.00% when the diameter was >4 cm. The USE stiffness score, strain ratio (SR) value, and MRI T2 value in the invasive group were all higher than those in the non-invasive group (P<0.05), with cutoff values of >3, >2.6, and >71.6, respectively, the achieving a specificity (series test) of 88.64%. ***Conclusion:*** USE combined with MRI T2 mapping enables multidimensional quantitative assessment of GCTTS invasiveness with excellent diagnostic performance. This approach provides a reliable reference for developing individualized surgical plans and holds significant clinical value.

INTRODUCTION

Giant cell tumor of the tendon sheath (GCTTS) is one of the most common soft tissue tumors of the hand and periarticular regions, accounting for 20%–30% of hand soft tissue tumors, mainly affecting young and middle-aged adults aged 20–50 years [1]. Although these tumors are predominantly benign, they exhibit significant local invasiveness. Approximately 60% of lesions invade joint capsules and ligaments, or even erode bone tissue, leading to joint pain, restricted mobility, and loss of joint function in severe cases, significantly reducing patients' quality of life [2]. Surgical resection is the primary treatment for GCTTS. However, the accuracy of preoperative assessment regarding the extent and severity of tumor invasion is critical to determining surgical outcomes [3]. Current clinical assessment of GCTTS invasiveness largely relies on conventional imaging examinations [4], each with inherent limitations. For instance, ultrasound, favored for its ease of use, real-time imaging, and non-invasive nature, is commonly employed for initial tumor localization and morphological observation. However, it only provides two-dimensional imaging and blood flow signals, making it difficult to accurately determine the depth of invasion into surrounding soft tissues and bone [5]. Conventional MRI sequences (T1-weighted imaging, T1WI; T2-weighted imaging, T2WI), though offer superior soft tissue resolution between tumors and surrounding structures, primarily provide qualitative assessments, which are highly subjective and cannot quantitatively reflect pathophysiological alterations in tumor tissues [6]. Previous studies have attempted to use single quantitative imaging techniques for GCTTS assessment, but most focused on differential diagnosis rather than invasiveness evaluation, with limited diagnostic performance [7, 8]. Therefore, seeking more effective preoperative diagnostic regimens for GCTTS remains a hot topic and challenge in clinics.

As is well established, ultrasound elastography (USE) can indirectly assess lesion invasiveness by detecting tissue stiffness, with higher tissue stiffness indicating greater tumor invasiveness [9]. Meanwhile, MRI T2 mapping enables quantitative measurement of tissue T2 values, reflecting water content and

[Downloaded from ijrr.com on 2026-11-08]

[DOI: 10.61186/ijrr.24.4.17]

collagen fiber distribution within tissues, which may correlate with the degree of tumor invasion [10]. Therefore, combining USE with MRI T2 mapping theoretically complements their respective limitations, enhancing diagnostic accuracy for GCTTS. However, to date, there are no published studies focusing on the combined application of these two quantitative imaging techniques for the preoperative evaluation of GCTTS invasiveness, and reliable clinical references are still lacking in practice.

Therefore, this study established a combined evaluation system integrating USE and MRI T2 mapping, leveraging the strengths of both techniques (real-time stiffness assessment by USE and quantitative histological feature analysis by MRI T2 mapping) to achieve a multidimensional, comprehensive assessment of GCTTS invasiveness. If validated, this approach may provide objective evidence for clinically precise preoperative determination of tumor invasion extent, assisting physicians in formulating rational surgical plans. The novelty of this study mainly includes the following aspects:

(1) For the first time, we explored the combined diagnostic value of USE and MRI T2 mapping for GCTTS invasiveness, and determined the optimal diagnostic thresholds and combined models;

(2) We clarified the correlation between the quantitative parameters of the two imaging techniques, providing a theoretical basis for their combined application;

(3) We verified the value of tumor size as a preliminary screening indicator for GCTTS invasiveness, which can assist clinicians in rapid risk stratification.

MATERIALS AND METHODS

Sample size estimation

Referencing previous similar studies [11], with postoperative pathological findings as the gold standard, we assumed a sensitivity of 85% and specificity of 80% for USE combined with MRI T2 mapping in assessing GCTTS invasiveness, with α set at 0.05 (two-tailed), β at 0.20 (80% test power), and an allowed dropout rate of 10%. Sample size estimation was performed using PASS 15.0 statistical software (Power Analysis and Sample Size Software, NCSS LLC, Kaysville, UT, USA), calculating a required sample size of 38 subjects per group.

Selection of study participants

Patients with suspected GCTTS who visited the Department of Orthopaedics of our hospital from January 2021 to December 2025 were selected as study participants. All patients were scheduled for surgical intervention. They completed preoperative USE and MRI T2 mapping examinations, with definitive diagnosis confirmed by postoperative pathological examination. This study was conducted in accordance with the Declaration of Helsinki, and the protocol was approved by the Medical Ethics Committee of Wuxi Ninth People's Hospital Affiliated to Soochow University (Approval No. 2021-9-112; Approval Date: September 15, 2021). All participants signed written informed consent forms before enrollment.

Inclusion and exclusion criteria

Inclusion criteria: (1) Aged 18–60 years, male or female; (2) Lesions located around joints such as hands, wrists, or feet, consistent with the clinical distribution characteristics of GCTTS; (3) No prior treatment affecting lesion tissue characteristics, including radiotherapy, chemotherapy, or needle biopsy; (3) Complete clinical records, enabling completion of two preoperative imaging studies and postoperative pathological follow-up; (4) Voluntary participation in this study, with informed consent signed.

Exclusion criteria: (1) Concurrent malignant tumors in other sites or multiple soft tissue tumors; (2) Contraindications for ultrasound examination (e.g., serious skin damage, infection) or MRI examination (e.g., metallic implants, claustrophobia, serious hepatic or renal insufficiency); (3) Extremely small lesion size (maximum diameter <0.5 cm), rendering elastography and quantitative T2 mapping impossible; (4) Incomplete postoperative pathological specimens or unclear pathological diagnosis; (5) Pregnant or lactating women; (6) Refusal to participate in this study or inability to complete follow-up.

Grouping

Using postoperative pathological examination results as the gold standard, the study participants were divided into invasive and non-invasive groups. Invasive group: Pathology confirmed tumor invasion of the surrounding joint capsule, ligaments, tendons, or bone (evidence of bone erosion or destruction). Non-invasive group: Pathology showed tumors confined within the tendon sheath without invasion of surrounding normal tissues. Grouping was determined by double-blind review of images by two experienced pathologists. In cases of disagreement, a consensus was reached through departmental consultation.

Ultrasound elastography examination

A LOGIQ™ E20 color Doppler ultrasound system (GE Healthcare, Chicago, IL, USA) equipped with a 5-12 MHz high-frequency linear array probe (GE Healthcare, Chicago, IL, USA) was employed for all examinations. Patients were positioned comfortably to ensure full exposure of the target lesion. Initially, conventional B-mode ultrasound scanning was

[Downloaded from ijrr.com on 2026-11-08]

[DOI: 10.61186/ijrr.24.4.17]

performed to assess and document baseline tumor characteristics, including size, shape, margin, internal echogenicity, and vascularity. Subsequently, real-time shear wave elastography was activated. The transducer was gently placed on the skin surface without applying compressive force to minimize tissue deformation. The region of interest (ROI) was set to encompass the entire tumor as well as a 5-mm peripheral zone of adjacent normal tissue. After ensuring image stability for 3–5 seconds, 3–5 representative elastographic images were acquired and stored for offline analysis. Two experienced radiologists, each with over 5 years of expertise in musculoskeletal ultrasound, independently evaluated the images under double-blind conditions. Tumor stiffness was qualitatively assessed using a standardized 5-point visual scoring system: 1 point-entirely green (soft); 2 points-predominantly green with minor blue areas (relatively soft); 3 points-approximately equal distribution of green and blue (moderate hardness); 4 points-predominantly blue with minor green regions (relatively hard); 5 points-uniformly blue (hard). Additionally, quantitative assessment was performed by calculating the strain ratio (SR) between the tumor and surrounding normal soft tissue.

MRI T2 mapping examination

All MRI examinations were conducted using a SIGNA Architect 3.0T MRI system (GE Healthcare, Chicago, IL, USA), with an appropriate radiofrequency coil selected according to the anatomical location of the lesion. Patients were positioned supine, and the affected area was immobilized to minimize motion artifacts. Standard imaging protocols included axial T1-weighted imaging (T1WI: repetition time, TR 500 ms, echo time, TE 15 ms) and T2-weighted imaging (T2WI: TR 3000 ms, TE 80 ms), with consistent parameters: slice thickness 3 mm, slice gap 0.3 mm, matrix size 256 × 256. T2 mapping was performed using a multi-echo spin-echo sequence with the following settings: TR 2000 ms, TEs at 10, 20, 30, 40, 50, and 60 ms, slice thickness 3 mm, slice gap 0.3 mm, matrix 256 × 256, field of view (FOV) ranging from 120 × 120 mm^2 to 180 × 180 mm^2, and acquisition time of 4-6 minutes. T2 maps were automatically generated using the scanner's built-in post-processing software. Two musculoskeletal radiologists, each with more than 5 years of diagnostic experience, independently analyzed the T2 maps in a blinded manner. Within the viable tumor parenchyma, three circular or oval regions of interest (ROIs; 5-10 mm^2 each) were manually placed, carefully avoiding areas of necrosis, calcification, and visible blood vessels. The mean T2 relaxation time (in milliseconds) was recorded for each ROI and averaged across the three measurements.

Outcome measures

Diagnostic efficacy of USE combined with MRI T2 mapping in assessing GCTTS invasiveness: The combined diagnosis employed the parallel test method (where positivity was defined as any single examination indicating invasiveness) and the serial test method (where positivity required both examinations to indicate invasiveness) to identify the optimal combined diagnostic model.

Statistical analysis

Data processing was conducted using SPSS 26.0 statistical software (IBM Corp., Armonk, NY, USA). Measurement data were first subjected to normality testing (Shapiro-Wilk test) and homogeneity of variance testing. Data that conformed to a normal distribution and exhibited homogeneity of variance were expressed as (`c±s), with intergroup comparisons performed using independent samples t -tests. Enumeration data were represented as [n(%)], and the χ^2 test was used for intergroup comparisons. The diagnostic threshold was determined using the receiver operating characteristic (ROC) curve analysis. $P<0.05$ was considered statistically significant.

RESULTS

Test results

Figure 1 shows the results of the MRI examination in one patient. Postoperative pathology confirmed invasiveness in 38 cases in the invasive group and 44 cases in the non-invasive group. No statistically significant differences were observed in general data such as age, gender, and lesion site between the two groups (all $P>0.05$), indicating good comparability between groups (table 1).

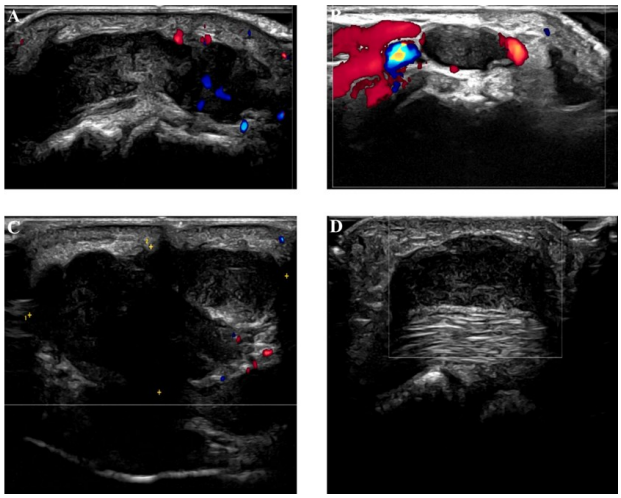


Figure 1. MRI examination images of a patient with pathologically confirmed invasive GCTTS. **(A)** Axial T1WI showing the soft tissue mass with isointense signal relative to muscle; **(B)** Axial fat-suppressed T2WI showing heterogeneous hyperintense signal of the mass with adjacent tissue invasion; **(C)** Axial T2 mapping pseudo-color map showing elevated T2 values within the tumor; **(D)** Postoperative HE staining image confirming invasive GCTTS.

[Downloaded from ijrr.com on 2026-11-08]

[DOI: 10.61186/ijrr.24.4.17]

Table 1. Comparison of general data between invasive group and non-invasive group.

	Invasive group (n=38)	Non-invasive group (n=44)	C2 (or t)	P
Age	35.74±10.43	34.73±8.43	0.485	0.629
Gender			0.020	0.888
male	17 (44.7)	19 (43.2)		
female	21 (55.3)	25 (56.8)		
Location of the lesion			0.413	0.814
hand	22 (57.9)	28 (63.6)		
wrist	10 (26.3)	9 (20.5)		
foot	6 (15.8)	7 (15.9)		

Note. n: number of cases; $\bar{x}\pm s$: mean ± standard deviation; χ^2: chi-square value; t: t value; P: P value.

Relationship between tumor size and invasiveness

The maximum diameter of tumors in the invasive group was (3.76±1.11) cm, which was significantly larger than that in the non-invasive group [(2.11±0.60) cm] (t=8.542, P<0.001). The patients were further categorized into three groups based on the maximum tumor diameter: <2 cm, 2-4 cm, and >4 cm. The results revealed that the incidence of invasiveness was 100.00% (15/15) for tumors >4 cm, 43.14% (22/51) for tumors 2-4 cm, and 6.25% (1/16) for tumors <2 cm. The risk of invasiveness increased significantly with the increase of tumor diameter (χ^2=28.735, P<0.001) (figure 2).

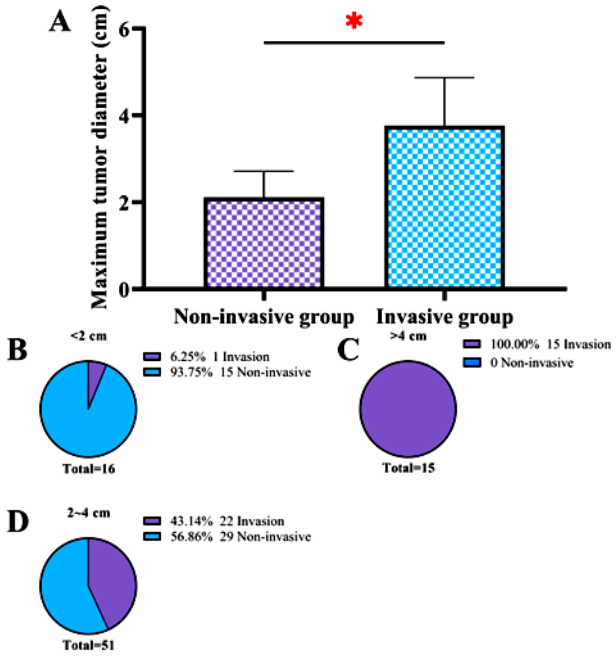


Figure 2. Distribution of invasive rate of GCTTS with different maximum diameters. **(A)** Box plot comparing the maximum tumor diameter between the invasive and non-invasive groups; Bar chart showing the invasion rates of GCTTS stratified by maximum tumor diameter <2 cm **(B)**, 2–4 cm **(C)**, >4 cm **(D)**. * Indicates P<0.05.

Comparison of imaging parameters between invasive and non-invasive groups

Compared with the non-invasive group, the invasive group had significantly higher USE stiffness scores (Z=-6.742, P<0.001), SR values (t=10.283, P<0.001), and MRI T2 values (t=9.874, P<0.001). Correlation analysis showed that USE stiffness score was positively correlated with MRI T2 value (r=0.633, 95%CI: 0.483-0.748, P<0.001), and SR value was also positively correlated with MRI T2 value (r=0.634, 95%CI: 0.484-0.748, P<0.001) (figure 3).

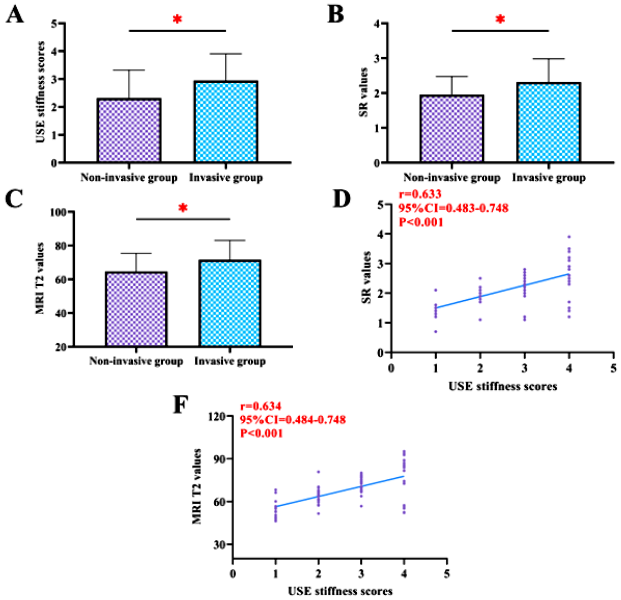


Figure 3. Comparison and correlation analysis of USE and MRI T2 mapping parameters between the invasive and non-invasive groups. **(A)** Bar chart comparing USE stiffness scores between the two groups; **(B)** Bar chart comparing SR values between the two groups; **(C)** Bar chart comparing MRI T2 values between the two groups; **(D)** Scatter plot showing the positive correlation between USE stiffness score and MRI T2 value; **(E)** Scatter plot showing the positive correlation between SR value and MRI T2 value. * Indicates P<0.05.

Analysis of critical values affecting test results

ROC curve analysis showed that when the cutoff values were set as USE stiffness score >3, SR >2.6, and MRI T2 value >71.6, the corresponding curves exhibited the highest Youden index (calculated as sensitivity + specificity - 1). Therefore, these thresholds were adopted for qualitative analysis (figure 4).

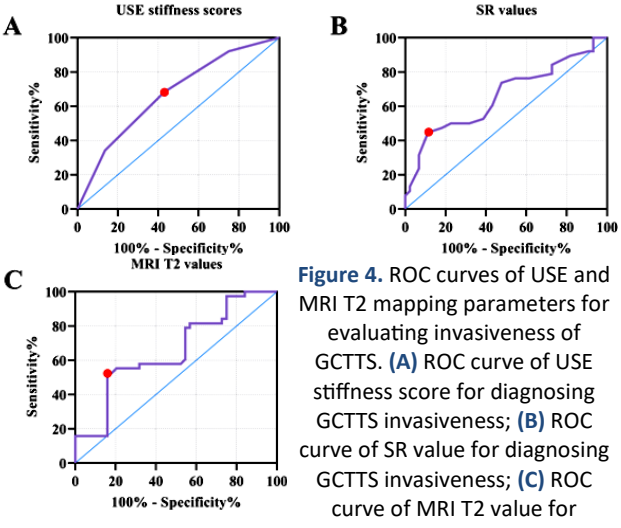


Figure 4. ROC curves of USE and MRI T2 mapping parameters for evaluating invasiveness of GCTTS. **(A)** ROC curve of USE stiffness score for diagnosing GCTTS invasiveness; **(B)** ROC curve of SR value for diagnosing GCTTS invasiveness; **(C)** ROC curve of MRI T2 value for diagnosing GCTTS invasiveness.

[Downloaded from ijrr.com on 2026-11-08]

[DOI: 10.61186/ijrr.24.4.17]

Comparison of diagnostic efficacy for assessing GCTTS invasiveness using different examination methods

Using postoperative pathological findings as the gold standard, the serial combined test showed significantly higher specificity and overall accuracy than single parameter examinations, with a specificity of 88.64% and an accuracy of 67.07% (table 2).

Table 2. Comparison of diagnostic efficacy of different examination methods in evaluating the invasiveness of GCTTS.

		Pathological examination			Sensitivity %	Specificity %	Accuracy %
		(+)	(-)				
Parallel test	(+)	24	21	45	63.16%	52.27%	57.32%
	(-)	14	23	37			
		38	44				
Serial test	(+)	16	5	21	42.11%	88.64%	67.07%
	(-)	22	39	61			
		38	44				

Note: (+): positive; (-): negative. Parallel test: combined positive is defined as any single test result meeting the positive threshold for invasiveness; Serial test: combined positive is defined as all single test results meeting the positive thresholds for invasiveness simultaneously.

DISCUSSION

The results of this study confirm that tumor size is closely associated with GCTTS invasiveness, and the combined application of USE and MRI T2 mapping can achieve high diagnostic specificity for GCTTS invasiveness, which provides a reliable imaging basis for preoperative assessment of GCTTS.

First, the association between tumor size and GCTTS invasiveness represents a key finding of this study. Mechanistically, as tumor volume increases, active cellular proliferation within the tumor leads to a dramatic rise in nutritional demands. When the blood supply within the tumor cannot meet metabolic needs, it invades surrounding tissues (e.g., joint capsules, ligaments, and bone) to establish new nutrient supply pathways. Concurrently, increased secretion of invasion-related factors like matrix metalloproteinases (MMPs) in the tumor microenvironment further promotes tumor infiltration into surrounding tissues [12, 13]. This study demonstrated that the incidence of invasion reaches 100.00% when the tumor's maximum diameter exceeds 4 cm, consistent with findings by Nakayama S *et al.* [14], which reported that large GCTTS lesions are more likely to invade adjacent bone tissue, confirming that tumor size serves as a preliminary screening indicator for GCTTS invasiveness. Furthermore, Li T X *et al.* [15] found that large GCTTS lesions can secrete higher levels of matrix metalloproteinases (MMPs) and transforming growth factor-β, which can degrade the extracellular matrix and promote tumor invasion; meanwhile, the increased mechanical pressure caused by enlarged tumor volume can disrupt surrounding tissue barriers [16, 17], further supporting the conclusions of this study

Second, the association between USE parameters and GCTTS invasiveness can be explained by pathophysiological mechanisms: Invasive GCTTS exhibits high tumor cell density, significant collagen fiber proliferation, and concomitant surrounding tissue fibrosis, leading to markedly increased tissue stiffness [18]. USE quantifies tissue stiffness through stiffness scores and SR values. Here, both stiffness scores and SR values were elevated in the invasive group, with optimal diagnostic thresholds of >3 and >2.6, respectively, which is similar to the results of Miao *et al.* on invasive soft tissue tumors [19]. However, single USE examination has certain limitations: the results may be affected by the operator's compression force, ROI selection, and lesion depth, which may lead to measurement bias [20], limiting its standalone diagnostic efficacy. The diagnostic value of MRI T2 mapping lies in its quantitative reflection of tissue microarchitecture [21]. During invasion, invasive GCTTS disrupts the anatomical structure of surrounding normal tissues, leading to enlarged interstitial spaces. Concurrently, the inflammatory response triggered by tumor cell proliferation increases tissue water content [22]. During invasion, invasive GCTTS disrupts the normal structure of surrounding tissues, leading to expanded interstitial space and increased tissue water content; meanwhile, the inflammatory response caused by tumor cell proliferation further elevates tissue water content [23], which is consistent with the findings of Wang *et al.* on T2 mapping for tissue microstructure assessment [24]. However, single T2 mapping examination may be affected by calcification, necrosis, and hemosiderin deposition in the lesion, which may lead to false negative results [25], which is the core reason why single examination cannot achieve optimal diagnostic efficacy. This is another reason why a single examination often fails to achieve optimal diagnostic efficacy. Additionally, the positive correlation between SR values and MRI T2 values suggests synchronous pathophysiological changes during tumor invasion. The collagen fiber proliferation induced by tumor invasion (increasing tissue stiffness and elevating SR values) and the increase in tissue water content (elevating T2 values) represent parallel pathological processes, both contributing to the progression of tumor invasion. This also highlights the complementary potential of the two imaging modalities, and our study further confirms that combined testing yields superior diagnostic performance compared to single approaches, which is consistent with the conclusion reported by Parravano *et al.* that combined multi-modal imaging diagnosis outperforms single examination [26]. Specifically, the parallel test enhances sensitivity, making it suitable for

[Downloaded from ijrr.com on 2026-11-08]

[DOI: 10.61186/ijrr.24.4.17]

preliminary screening of invasiveness; the serial test achieved a high specificity of 88.64%, which is applicable for scenarios requiring precise exclusion of invasiveness, such as formulating surgical plans to preserve joint function as much as possible. This finding aligns with the conclusion reported by Samora NL *et al.* that combined imaging diagnosis outperforms single approaches [27], confirming the clinical value of the combined assessment system.

Limitations

However, as a single-center retrospective study, the sample size of this study is limited, and there may be selection bias. The generalizability of these findings requires validation through multicenter, large-sample studies. Second, imaging results depend on the physician's expertise in operation and interpretation. Although double-blind reading was employed, the operating procedures were not standardized. Differences in equipment models and parameter settings may compromise result consistency. Third, the correlation of tumor pathological grading and immunohistochemical markers (e.g., CD68, Ki-67) with imaging indicators was not analyzed, thus failing to clarify the underlying molecular mechanisms linking these indicators to tumor proliferative activity and invasiveness. Subsequently, we need to incorporate other imaging modalities (e.g., contrast-enhanced MRI, CT) for comparative analysis to determine the advantages and disadvantages of this combined system versus alternative approaches.

CONCLUSION

GCTTS tumor size is closely correlated with invasiveness. USE and MRI T2 mapping can effectively quantify tumor invasiveness, and there is a synergistic correlation between the indicators of the two techniques. The combined diagnostic system outperforms individual examinations, particularly demonstrating high specificity (93.18%) in serial testing, which provides objective evidence for precise preoperative clinical assessment and aids in developing individualized surgical plans. Multi-center, large-sample, and prospective studies are needed to further verify its reliability and generalizability.

***Ethical Approval*:** The study protocol was approved by the Ethics Committee of Wuxi Ninth People's Hospital Affillated to Soochow University (NO. 2021-9-112).

***Conflicts of Interest*:** The authors report no conflict of interest.

***Availability of data and materials*:** The data that support the findings of this study are available from the corresponding author upon reasonable request.

***Funding*:** No funds, grants, or other support was received.

***Author contributions*:** QL.C. designed the study, M.C. and YX.J. wrote and revised manuscript, QL.C. and M.C. collected and analyzed data, M.C. and YX.J. made equal contributions in this work as co-first authors. All authors read and approved the final submitted manuscript.

REFERENCES

1. Kager M, Kager R, Falek P, Falek A, *et al.* (2022) Tenosynovial giant cell tumor. *Folia Med Cracov,* ***62****(2): 93-107.*
2. Huang CG, Li MZ, Wang SH, Tang XQ, *et al.* (2023) Giant cell tumor of tendon sheath: A report of 216 cases. *J Cutan Pathol,* ***50****(4): 338-42.*
3. Suneja P, Diwaker P, Ranjan K (2023) Cytomorphologic panorama of giant cell tumour of tendon sheath. *Diagn Cytopathol,* ***51****(12): 772-8.*
4. Edupuganti N and Dyer JM (2024) Subungual Giant Cell Tumor of the Tendon Sheath: An Unusual Location. *J Clin Aesthet Dermatol,* ***17****(12): 25-7.*
5. Verdaguer-Faja J, Redondo Bellon P, Garcia-Martinez FJ (2024) Ultrasound Imaging in Giant Cell Tumor of the Tendon Sheath. *Skin Res Technol,* ***30****(9): e70066.*
6. Liu X, Xu H, Jiang T, Zhang B, *et al.* (2021) MRI and (18)F-FDG PET/CT findings of a giant cell tumor of the tendon sheath of the knee joint (pigmented villonodular synovitis): A case report and literature review. *Hell J Nucl Med,* ***24****(2): 149-54.*
7. Khurana A, Singh JP, Preeti, Littlefield Z, *et al.* (2023) Demystifying Giant Cell Tumours of Tendon Sheath (GCTTS): A Case Series of 18 Cases with Review of Literature. *Indian J Orthop,* ***57****(11): 1858-73.*
8. Michailidis A, Tsifountoudis I, Kitridis D, Karagergou E, *et al.* (2025) Role of MRI and surgical excision in long-standing diffuse-type GCTTS of the flexor tendon sheath. *Radiol Case Rep,* ***20****(3): 1368-73.*
9. Giambini H and An KN (2022) Ultrasound elastography for hand soft tissue assessment. *Hand Clin,* ***38****(1): 119-28.*
10. Leskinen HPP, Tuppurainen J, Jantti J, Makela JTA, *et al.* (2025) Orientation-Independent T2 Mapping Enhances MRI-Based Cartilage Characterization. *Ann Biomed Eng,* ***53****(9): 2120-30.*
11. Ertem H, Seluk S, Orman O, Ozturk K, Baydar M (2024) The effect of surgical factors on recurrence of tendon sheath giant cell tumours. *J Hand Surg Eur Vol,* ***49****(8): 977-80.*
12. Sonkusale A, Gandhi P, Maurya V, Giri V (2023) Giant cell tumor of flexor pollicis longus tendon sheath: An uncommon case report and literature review. *J Orthop Case Rep,* ***13****(8): 32-5.*
13. Chan AS, Katiyar V, Dy P, Singh V (2023) Updates on the treatment of tenosynovial giant cell tumor. *Hematol Oncol Stem Cell Ther,* ***16*** *(4): 307-15.*
14. Nakayama S, Nishio J, Aoki M, Nabeshima K, Yamamoto T (2022) t (1;2)-Positive localized tenosynovial giant cell tumor with bone invasion. *In Vivo,* ***36****(5): 2525-9.*
15. Li T, Xiong Y, Li J, Tang X, *et al.* (2024) Mapping and analysis of protein and gene profile identification of the important role of transforming growth factor beta in synovial invasion in patients with pigmented villonodular synovitis. *Arthritis Rheumatol,* ***76****(11): 1679-95.*
16. Wu J, Zhang F, Huang Y, Wei L, *et al.* (2024) Predictive value of cyst/tumor volume ratio of pituitary adenoma for tumor cell proliferation. *BMC Med Imaging, 24(1): 69.*
17. Pikuniene I, Straksyte V, Basevicius A, Zilinskas J, *et al.* (2023) Prognostic value of tumor volume, tumor volume reduction rate and magnetic resonance tumor regression grade in rectal cancer. *Medicina (Kaunas, Lithuania),* ***59****(12): 2194.*
18. Huang Q, Wu X, Xia Q, Xie Z, *et al.* (2025) Diffuse-type tenosynovial giant cell tumor invading the temporal bone: Three cases. *Ear Nose Throat J,* ***104****(7): NP450-NP5.*
19. Miao L, Jiang J, Li J, Liu H, *et al.* (2025) Whole-tumor histogram analysis of synthetic MRI for the differentiation of benign and malignant soft-tissue tumors: A preliminary study. *Eur Radiol,* ***35*** *(12): 7888-99.*

[Downloaded from ijrr.com on 2026-11-08]

[DOI: 10.61186/ijrr.24.4.17]

20. Wu CH, Chiu YH, Chang KV, Wu WT, Ozcakar L (2022) Ultrasound elastography for the evaluation of plantar fasciitis: A systematic review and meta-analysis. *Eur J Radiol,* ***155****: 110495*.
21. Agergaard AS, Malmgaard-Clausen NM, Svensson RB, Nybing JD, *et al.* (2021) UTE T2* mapping of tendinopathic patellar tendons: an MRI reproducibility study. *Acta Radiol,* ***62****(2): 215-24*.
22. Doroszko M, Stockgard R, Uppman I, Heinold J, *et al.* (2025) The invasion phenotypes of glioblastoma depend on plastic and reprogrammable cell states. *Nat Commun,* ***16****(1): 6662*.
23. Cheng X, Cao Y, Liu X, Li Y, *et al.* (2024) Single-cell and spatial omics unravel the spatiotemporal biology of tumour border invasion and haematogenous metastasis. *Clin Transl Med,* ***14****(10): e70036*.
24. Wang L, Luo R, Chen Y, Liu H, *et al.* (2023) Breast Cancer Growth on Serial MRI: Volume Doubling Time Based on 3-Dimensional Tumor Volume Assessment. *J Magn Reson Imaging,* ***58****(4): 1303-13*.
25. Khil EK, Cha JG, Kim SJ, Yoon YS (2025) Quantitative T2 mapping analysis with MRI of talar cartilage in ankle trauma: A study based on Lauge-Hansen classification and anatomical locations. *Korean J Radiol,* ***26****(5): 435-45*.
26. Parravano M, Cennamo G, Di Antonio L, Grassi MO, *et al.* (2024) Multimodal imaging in diabetic retinopathy and macular edema: An update about biomarkers. Surv Ophthalmol, **69**(6): 893-904.
27. Samora NL, Al Hussein Al Awamlh B, Tosoian JJ (2023) Combined use of magnetic resonance imaging and biomarker testing to detect clinically significant prostate cancer. *Urol Clin North Am,* ***50*** *(1): 91-107*.

[Downloaded from ijrr.com on 2026-11-08]

[DOI: 10.61186/ijrr.24.4.17]

[DOI: 10.61186/ijrr.24.4.17] [Downloaded from ijrr.com on 2026-11-08]